Journal of Controlled Release 194 (2014) 138–147

Contents lists available at ScienceDirect

Journal of Controlled Release

journal homepage: www.elsevier.com/locate/jconrel

PLGA nanoparticles loaded with host defense peptide LL37 promote wound healing

Kiran Kumar Chereddy [a], Charles-Henry Her [a], Michela Comune [b], Claudia Moia [c], Alessandra Lopes [a], Paolo E. Porporato [d], Julie Vanacker [a], Martin C. Lam [e], Lars Steinstraesser [e], Pierre Sonveaux [d], Huijun Zhu [c], Lino S. Ferreira [b], Gaëlle Vandermeulen [a,1], Véronique Préat [a,*,1]

[a] Université catholique de Louvain, Louvain Drug Research Institute (LDRI), Advanced Drug Delivery and Biomaterials, Avenue E. Mounier 73 box B1.73.12, 1200 Brussels, Belgium
[b] Center of Neurosciences and Cell Biology, University of Coimbra, 3004-517 Coimbra, Portugal
[c] Environmental Science and Technology Department, School of Applied Sciences, Cranfield University, Bedford MK43 0AL, UK
[d] Université catholique de Louvain, Institut de Recherche Expérimentale et Clinique (IREC), Pole of Pharmacology, Avenue Emmanuel Mounier 52 box B1.53.09, 1200 Brussels, Belgium
[e] Department of Plastic, Reconstructive and Aesthetic Surgery, European Medical School at the Carl von Ossietzky University of Oldenburg, Evangelisches Krankenhaus, Steinweg 13-17, 26122 Oldenburg, Germany

ARTICLE INFO

Article history:
Received 13 May 2014
Accepted 14 August 2014
Available online 27 August 2014

Keywords:
Wound healing
Poly(lactic-co-glycolic acid) (PLGA)
Host defense peptide
LL37
Lactate
Nanoparticles

ABSTRACT

Wound treatment remains one of the most prevalent and economically burdensome healthcare issues in the world. Poly (lactic-co-glycolic acid) (PLGA) supplies lactate that accelerates neovascularization and promotes wound healing. LL37 is an endogenous human host defense peptide that modulates wound healing and angiogenesis and fights infection. Hence, we hypothesized that the administration of LL37 encapsulated in PLGA nanoparticles (PLGA-LL37 NP) promotes wound closure due to the sustained release of both LL37 and lactate. In full thickness excisional wounds, the treatment with PLGA-LL37 NP significantly accelerated wound healing compared to PLGA or LL37 administration alone. PLGA-LL37 NP-treated wounds displayed advanced granulation tissue formation by significant higher collagen deposition, re-epithelialized and neovascularized composition. PLGA-LL37 NP improved angiogenesis, significantly up-regulated IL-6 and VEGFa expression, and modulated the inflammatory wound response. *In vitro*, PLGA-LL37 NP induced enhanced cell migration but had no effect on the metabolism and proliferation of keratinocytes. It displayed antimicrobial activity on *Escherichia coli*. In conclusion, we developed a biodegradable drug delivery system that accelerated healing processes due to the combined effects of lactate and LL37 released from the nanoparticles.

1. Introduction

Wound treatment and its medical complications remain one of the most prevalent and economically challenging healthcare issues in the world. The annual wound care products market has reached to $15.3 billion by 2010 and still the need for post-surgical wound care is sharply on the rise. In the USA alone there are more than 100 million wounds annually, including surgical incisions, trauma, burns, blast injuries, diabetic ulcers, ostomies, bedsores, and more [1,2]. Acute wounds heal in a very orderly, timely and efficient manner characterized by four distinct, strictly connected but overlapping phases: hemostasis, inflammation, proliferation and remodeling. Any disturbances in these phases may result in an incomplete and improper restoration of the injured tissue [3]. In these severe clinical conditions wound repair may fail to proceed, leading to chronic non-healing wounds. Current treatment options are limited, costly, and inefficient. As a result, the development of new therapeutics is absolutely necessary to satisfy the unmet clinical need.

One of the simple and pragmatic solutions to faster wound healing process was the application of exogenous lactate that accelerates angiogenesis, activation of procollagen factors and recruitment of endothelial progenitor cells in wounds. Utilization of poly (lactic-co-glycolic acid) (PLGA) is one of the strategies to supply lactate sustainably [4]. Moreover, PLGA is biodegradable, biocompatible, has versatile degradation kinetics and approved by the European Medical Agency and Food and Drug Administration as an excipient for parenteral products [5]. Thus the key advantage of PLGA drug delivery systems is the polymer can perform the dual roles: being a wound healing agent itself and its capability to release loaded drugs sustainably to the wound.

LL37 belongs to antimicrobial peptides/host defense peptides that are part of the innate immune system and represent the first line of defense against many invading pathogens [6]. hCAP-18/LL37 is up to now the only antimicrobial peptide of the cathelicidin family identified in humans. LL37 has been detected in an inactive proform in several

* Corresponding author. Tel.: +32 2 764 7309; fax: +32 2 764 7398.
E-mail address: veronique.preat@uclouvain.be (V. Préat).
[1] Equal contribution.

http://dx.doi.org/10.1016/j.jconrel.2014.08.016
0168-3659/

types of cells such as neutrophils, mast cells, monocytes, macrophages, NK cells, γδ cells, B cells, dermal epithelial cells and keratinocytes, inflamed skin and blister fluids. Any infection or tissue and cell damage that occurs during the wound may activate TLR(s) and/or an alteration in the cytokine milieu, which provides a trigger that activates the cell to degranulate. This leads to the release of the inactive hCAP18 precursor in the extracellular environment, where it can be processed by specific proteases into the active 37 amino acid long LL37 peptide [7–9]. LL37 exerts different immunomodulatory functions like broad antimicrobial activity, antiviral and antifungal activity, endotoxin-binding properties, modulation of pro-inflammatory response, chemotaxis, influence on cell proliferation and differentiation, promotion of wound healing and angiogenesis, *etc.* [10]. The major difficulty associated with LL37 administration is its immediate degradation in the wound environment and thus the treatment requires high dose and dosing frequency of LL37 [11] or gene therapy [12] to produce the therapeutic effect.

PLGA nanoparticles (NP) have been successfully proved to be efficient carriers for large biomolecules such as vaccines and proteins for the treatment of various ailments [5,13]. Hence, we hypothesized that the administration of LL37 encapsulated in PLGA nanoparticles (PLGA-LL37 NP) could efficiently deliver the LL37 and accelerate wound closure through different mechanisms due to the encapsulated LL37 and lactate released from PLGA. Thus, we present the PLGA-LL37 NP for the active healing of dermal wounds and study their mechanisms of action.

2. Materials and methods

2.1. PLGA-LL37 nanoparticle preparation

LL37 loaded PLGA (50:50, Mw 7000–17,000, acid terminated, Boehringer Ingelheim GmbH, DE) nanoparticles were prepared by W/O/W emulsion–solvent evaporation technique with a few modifications from the literature [14]. Briefly, 20 mg of PLGA polymer was dissolved in 1 ml dichloromethane (HPLC grade, Sigma-Aldrich, DE). 20 μg of LL37 (95.0% pure, Caslo ApS, DK) (peptide sequence LLGDF FRKSKEKIGKEFKRIVQRIKDFLRNLVPRTES, theoretical molecular mass 4493.37) in 20 μl sterile water, was added to PLGA solution and sonicated (Branson sonifier, USA) at 70 W for 15 s to form W/O primary emulsion. The primary emulsion was further emulsified with 2 ml of 1% (*w*/*v*) polyvinyl alcohol (PVA, Mw 13,000–23,000, Sigma-Aldrich, DE) dissolved in sterile water and again sonicated at 70 W for 15 s to generate the W/O/W emulsion. This emulsion was added drop by drop to 50 ml of 0.3% (*w*/*v*) PVA and stirred at 600 rpm and 37 °C for 1 h on a water bath. The nanoparticle suspension was then washed twice in sterile water by centrifugation (Avanti-JE centrifuge, Beckman coulter, USA) for 40 min at 22,000 ×*g* and 4 °C. Supernatants were collected to evaluate encapsulation efficiency of LL37. Empty nanoparticles (PLGA NP) were prepared with the same procedure except the addition of LL37 during the preparation of formulation. All the particles were then freeze dried and lyophilized (Labconco, USA) for 24 h and stored at 4 °C until further use. All the materials used were sterilized and the procedures were performed under laminar flow.

2.2. PLGA-LL NP characterization

2.2.1. Particle size, poly dispersity and zeta potential

The particle size and poly dispersity index (PDI) of PLGA NP and PLGA-LL37 NP were measured by dynamic light scattering and the zeta potential was determined using a zeta potential analyzer (NanoSizer Zeta Series, Malvern Instruments, UK).

2.2.2. LL37 encapsulation efficiency

Encapsulation efficiency estimated the amount of LL37 encapsulated in PLGA-LL37 NP. Supernatants were used to measure the non-encapsulated LL37 and 1 mg of lyophilized PLGA-LL37 NP was dissolved in 1 ml of chloroform and 1 ml of water to collect the encapsulated LL37. LC-MS (Q-Exactive-ESI MS, Thermo Fischer, BE) was used to quantify the LL37. The HPLC column is an XBridge C18 150 × 2.1 mm (Waters, BE) and the elution flow rate was 200 μl/min. The gradient was maintained for 1 min at 90% H_2O (0.1% HCOOH–1% CH_3CN) and 10% CH_3CN and then 24 min at 5% H_2O (0.1% HCOOH–1% CH_3CN) and 95% CH_3CN. 10 μl of the sample was injected in the Q-Exactive mass spectrometer (HPLC-ESI, Thermo Fischer, BE) and the most abundant $[749.77269]^{6+}$ ion was analyzed in the positive and selective ion mode. Full scanning of *m*/*z* was performed to check any chemical modification of peptide. A calibration curve was plotted by LL37 peptide from 1 ng/ml to 25,000 ng/ml. LL37 was quantified and the encapsulation efficiency of LL37 is given by [LL37 encapsulated/LL37 initial] × 100 and thus LL37 recovery was calculated.

2.3. In vitro drug release profile and stability studies

Four milligrams of dried PLGA-LL37 NP was transferred into 5 ml glass vials sealed with plastic caps and was kept in a stability chamber with a temperature of 25 ± 2 °C and an RH of 60 ± 5%. On days 0, 5, 15 and 30, the formulations were measured for changes in particle size and morphology, PDI and drug loading as described in Sections 2.2.1 and 2.2.2 [15]. Four milligram PLGA-LL37 NP (containing 4.04 μg LL37) were dispersed in 500 μl of phosphate buffer solution (PBS) (Gibco, BE) and pelleted by centrifugation at 12,000 ×*g* for 10 min and placed at room temperature (RT). On days 0, 1, 2, 3, 4, 7, 9, 12 and 14 the supernatant (200 μl) was aspirated and stored at −80 °C and the same amount fresh PBS added to the solution [16]. The amount of released LL37 per time point was determined as described in Section 2.2.2 and expressed as cumulative LL37 release %. Ten milligram PLGA-LL37 NP were dispersed in 10 ml of PBS. The NP were incubated at RT and stirred for 15 days. On days 0, 5, 10 and 15 samples were harvested and filtered using ultracentrifugation filter tubes (10 kDa cutoff, VWR, BE) before measuring the lactate concentration with a CMA600 enzymatic analyzer (Aurora Borealis, NL) according to manufacturer's instructions. The amount of released lactate per time point was expressed as μg/mg. This test is specific to L-lactate [4].

2.4. In vivo wound healing assay

Six to seven week old RjHan:NMRI female mice (Janvier, BE) were randomly selected and grouped following the standardized animal experimental protocols. Animals were from the same breed, age and near body weight (as delivered by supplier). Temperature and RH were maintained constant in the animal facility. Mice were anesthetized with isoflurane and the dorsal area was shaved using a depilatory cream (Veet for sensitive skin, BE) a day before the surgery to avoid the irritation. Two 0.5-mm-thick silicone (Grace biolabs, UK) donut-shaped splints (OD = 20 mm, ID = 10 mm) were fixed on either side of the dorsal midline, approximately 3.5 cm distal from the ears and positioned with 6–0 nylon sutures (Monosof, USA). Full-thickness excisional wounds were created using an 8 mm round skin biopsy punch (Kai Europe GMBH, DE), centered within each splint [17,18]. In order to investigate re-epithelialization as a major factor in wound healing, splints were used to avoid skin contraction. There were no infection of the wounds and drop-outs during the study. The animal studies were approved by the animal care and ethical committee of medical sector, Université catholique de Louvain.

2.4.1. In vivo dose–response curve for wound healing activity

Mice were randomly assigned into groups ($n = 5$) and treated with either (i) 1, 2.5, 5, 7.5 or 10 μg of LL37 (ii) 0.5, 1.25, 2.5, 3.75 or 5 mg of D, L-lactic acid (USA pharmacopeia grade, Sigma, DE) (iii) 1, 2.5, 5, 7.5 or 10 mg of PLGA NP (iv) 1, 2.5, 5, 7.5 or 10 mg of PLGA-LL37 NP (v) untreated, to plot the dose–response curves. Two wounds were made on each mouse and each wound received a different treatment

intradermally at 4 sites around the each wound. Wounds were covered with transparent sterile adhesive bandage (IV3000, Smith & Nephew, UK) followed by adhesive fabric tape (BSN medical, FR). On different days, wounds were digitally photographed by Leica IC80 HD camera (Leica, CH). Optical zoom was maintained identical throughout the experiments. Wound areas were quantified using Jmicro Vision software (University of Geneva, CH). Wound sizes are expressed as percentage of the respective initial wound.

2.4.2. Study of mechanisms of action

Eight mice were randomly assigned per group and wounds were administered with only vehicle (0.9% *w*/*v* NaCl, Mini-Plasco, BE), 5 μg LL37, 5 mg PLGA NP, 5 mg PLGA-LL37 NP (equivalent to 5 mg PLGA and 5 μg LL37) in 30 μl of vehicle by a sterile insulin syringe (BD medical, FR). As a positive control, one group of mice was administered with 50 μg of plasmid encoding hCAP18/LL37 (pLL37) (diluted in sterile PBS to a total volume of 80 μl). Wound and the surrounded skin were placed in between a 2 mm spaced plate-electrode and the electroporation was performed by a Cliniporator system (IGEA, IT). One pulse 700 V/cm 100 μs and one 200 V/cm 400 ms electric pulses, without pause in between, were applied. A conductive gel was applied to ensure electrical contact with the skin (Aquasonic 100 ultrasound transmission gel, Parker lab, USA) [18]. Wound treatment and area quantification were performed as described in Section 2.4.1. On days 5 and 10, three animals per group were sacrificed and wounds along with surrounding tissue were collected and bisected into two halves for further experiments. Remaining animals were sacrificed on day 19. All the *in vivo* data have been cumulated and hence $n = 10–13$.

2.5. Histology and Immunohistochemistry

2.5.1. Hematoxylin and eosin (HE) and Masson's trichrome (MT) staining

The wound halves ($n = 3$) were immediately fixed with paraformaldehyde (4% in PBS, 0.01 M, pH 7.4) and after 24 h the samples were transferred to PBS buffer at 4 °C. Wound tissue was embedded in paraffin blocks and sequentially sectioned at 5 μm using a MICROM 17 M325 microtome (Thermo Fisher Scientific, DE). Skin sections were stained with HE to assess the predominant stages of healing and with MT green staining to study the extent of collagen deposition in healed tissue during the course of wound healing. Images were taken with an AxioCam camera on an Axioplan microscope (Carl Zeiss GmbH, DE). All histological analyses were performed on at least 3 wounds per group per time point and images presented are representatives of all replicates.

2.5.2. CD-31 marking

The wound halves ($n = 3$) were embedded in Tissue-Tek O.C.T. compound (Sakura Finetek, CA) and frozen. Sections were cut at 10 μm thickness using a cryostat (Leica Microsystems, CH). An antibody directed against the murine endothelial cell surface marker (CD-31) was used to determine the extent of endothelial cell colonization in the wound sections. After permeabilization (Triton X-100 (Sigma-Aldrich, DE) 0.1% (*v*/*v*) in PBS) and blocking (5% (*w*/*v*) BSA in PBS), the primary antibody (rat anti-CD-31 (1:50), BD Biosciences, USA) was applied for 1 h at 37 °C. Secondary antibody (Alexa Fluor 568 goat anti-rat (1:500), Invitrogen, BE) was used to visualize the antigen. Finally, sections were incubated with DAPI (Invitrogen, BE) (50 ng/ml) for 5 min to visualize the cell nuclei. Images of entire sections were acquired by a MIRAX microscope (Zeiss, DE). Red fluorescence of CD-31 + (Alexa Fluor 568) was quantified on whole sections using a script of FRIDA software (developed by Johns Hopkins University, USA). Results were expressed as percentage of red pixels over the total amount of pixels within the analyzed surface [19].

2.6. Collagen (Sircol) assay

The homogenate of wound tissue was used to measure the total acid-soluble collagen (types I–V) colorimetrically using a Sircol Collagen Assay kit (Biocolor, UK) following the manufacturer's instructions. Briefly, wound tissue sample ($n = 3$) of the 10th day, was homogenized in lysis buffer (100 mM potassium phosphate, 0.1% Triton X-100, 2 mM dithiothreitol, 100 μg/ml phenylmethylsulfonylfluoride, pH 7.8) and tissue debris was removed by centrifugation at 12,000 ×*g* for 10 min (Biofuge 15 R, Heraeus Sepatech, USA). Sircol dye reagent was added to tissue extracts, stirred for 30 min at room temperature and centrifuged at 12,000 ×*g* for 10 min. Absorbance of the bound dye was measured at 560 nm in a spectrophotometer (Spectramax M2e & program SoftMax Pro, USA). The amount of collagen protein in skin samples was adjusted to the amount of total protein using the BCA Protein Assay kit. Collagen concentrations were expressed as μg collagen per gram of total protein [20].

2.7. q-PCR of IL-6 and VEGFa

Total RNA was isolated from collected wounded tissues using TRIzol® reagent (Ambion, Invitrogen, BE). RNA samples were subjected to DNase I (Promega, USA) treatment to remove genomic DNA contamination in the presence of RNase inhibitor. The quantity of RNA was evaluated by a nanospectrophotometer (NanoDrop 2000, Thermo Scientific, DE) and the final concentration of RNA was adjusted to 1 μg/3 μl. 1 μg RNA was reverse transcribed using first standard synthesis system (SuperScript™, Invitrogen, BE) and oligo (dT) primer (Eurogentec, BE) following the supplier protocol and stored at −20 °C. SYBR green real-time qPCR (GoTaq qPCR MasterMix kit, Promega, A6000) was conducted with primers designed based on murine mRNA sequences using PerlPrimer on a StepOne Plus Real-Time PCR System (Applied Biosystems, BE) (Table 1 of supplementary data 1). Every sample was tested in duplicate. Melting curves were analyzed for each run to assess the presence of unspecific PCR products. A blank was included in each assay run. β-actin served as the housekeeping gene. The results were analyzed with StepOne Software V2.1. The mRNA expression of IL-6 and VEGFa genes was calculated relative to the expression of corresponding β-actin, according to the delta-delta Ct method.

2.8. Myeloperoxidase (MPO) assay

Briefly, wound tissues from each group ($n = 3$) on days 5 and 10 were collected as described in Section 2.4 and snap frozen in liquid N_2 and stored for later assessment. Tissue was placed in hexadecyltrimethylammonium bromide (HTAB) buffer (0.5% HTAB in 50 mM potassium phosphate buffer, pH 6) on ice and gently homogenized. The homogenate was centrifuged (Allegra X-15R, Beckman Coulter, USA) at 2000 ×*g* for 10 min and subsequently centrifuged (Biofuge 15 R, Heraeus Sepatech, USA) at 18,400 ×*g* for 20 min at 4 °C. The supernatant (7 μl) was added to 96-well plates (Nunc, DK) and followed by 200 μl of a 50 mM potassium phosphate buffer containing 0.167 mg/ml *O*-dianisidine (Sigma-Aldrich, DE) and 500 ppm hydrogen peroxide (Merck, DE) in each well. Samples were analyzed in triplicate. Absorbances of the supernatants were measured spectrophotometrically at 460 nm for 30 min. The results were expressed as MPO units per gram of tissue, and one unit of MPO activity was defined as the amount that degrades 1 mmol/min of hydrogen peroxide at 25 °C [21].

2.9. Cellular assays

HaCaT (ECACC, UK) and BJ fibroblast cells (ATCC 2522, UK) were cultured in DMEM/F-12 with L-Glutamine and 15 mM HEPES, supplemented with 10% (*v*/*v*) FBS (Invitrogen, UK). Macrophage cell culture (J774A.1, Cell line service, DE) was cultured on Dulbecco's Modified

Eagle's Medium (DMEM) (Sigma, DE) supplemented with a solution of antibiotics (penicillin and streptomycin—1%, *v*/*v*) and fetal bovine serum (10%, *v*/*v*, FBS) (Invitrogen, BE) until achieving 90% of confluence before the harvest. Cells were recovered from tissue culture flasks using a sterile cell scraper and were passaged in a ratio of 1:3. Cells were grown in an atmosphere of 5% CO_2/95% air (*v*/*v*) at 37 °C. *Escherichia coli* cells (ATCC 25922, UK) were grown on LB plates (Luria–Bertani broth with 1.5% agar) at 37 °C.

2.9.1. Proliferation assay

HaCaT cells and BJ fibroblasts (3000 cells/well, $n = 4$) were seeded in a 96-well plate (Corning, UK) and cultured at 37 °C in the media of concentrations 500 ng/ml LL37, 500 μg/ml PLGA NP and 500 μg/ml PLGA-LL37 NP. After 4 day incubation, cell lysates were prepared by the addition of 1% Triton X-100 followed by 3 freeze–thaw cycles. Double-stranded DNA (dsDNA) content of cell lysates was measured by Quant-iT dsDNA high-sensitivity assay kit (Invitrogen, BE) [16].

2.9.2. In vitro wound healing assay

IBIDI culture-inserts (IBIDI, DE) plated on 24 well plate (Nunclon, DK) were used to perform the *in vitro* wound healing assay [18]. HaCaT cells (15,000 cells in 80 μl of medium/side of IBIDI insert) were seeded and cultured in growth media until confluence (24 h). IBIDI culture inserts were removed and the two cell islands were washed with PBS to remove debris. Cells were cultured at 37 °C in the medium of concentrations 500 ng/ml LL37, 500 μg/ml PLGA NP and 500 μg/ml PLGA-LL37 NP and untreated as control. Photographs of the *in vitro* wounds ($n = 3$) were taken at the beginning (0 h) and every 6 h for 24 h with a microscope (5× lens, Leica DFC 295, CH). The width of the IBIDI separation wall was measured using Jmicro Vision.

2.9.3. Cytotoxicity assay

Cytotoxicity of the formulations on HaCaT cells was evaluated using the MTT and LDH assays. HaCaT cells (3000/well) were seeded in a 96-well plate and maintained for 24 h. Cells were treated with media of concentrations 500 ng/ml LL37, 500 μg/ml PLGA NP and 500 μg/ml PLGA-LL37 NP for 90 min. Cells with 1% Triton X-100 and with medium only served as positive and negative controls respectively. For MTT assay, cells were incubated for 4 h with the medium containing 0.5 mg/ml MTT (3-(4,5-dimethylthiazol-2-yl)-2,5-diphenyltetrazolium bromide) (Sigma-Aldrich, DE). The medium was then removed and 100 μl DMSO was added to dissolve the purple formazan crystals. Absorbance was measured at 570 nm using Varian Flash plate reader (Thermo Fisher Scientific, USA). For LDH assay, the protocol of the cytotoxicity detection kit-LDH (Version 6, Roche Applied Science, USA) was followed. Briefly, cells were centrifuged (Heraeus Mega16 centrifuge, Thermo scientific, UK) for 5 min at 250 ×*g*. 50 μl of supernatant medium from each well was collected into another 96-well plate and added with 100 μl of freshly prepared reaction mixture and incubated for 30 min at 25 °C in dark. Absorbance was measured at 492 nm. Absorbance from medium was subtracted and cell viability and mortality were expressed as percentage of controls ($n = 4$).

2.9.4. q-PCR analyses of IL-6 and TNFα in macrophages

Macrophage cells (passage 42) were seeded at a density of 2×10^4 cells per well in a 24 well plate (Costar, Sigma Aldrich, PT) for 24 h and incubated with media containing LL37 (100 and 300 ng/ml), PLGA NP and PLGA-LL37 NP (100 and 300 μg/ml) for 24 h. Cells were lysed with TRIzol® reagent and then stored at −80 °C. Following the manufacturer's instructions, total RNA was isolated by an RNeasy Mini Kit (QIAGEN, PT). The quality and quantity of RNA were evaluated by spectrophotometric analysis. cDNA was synthesized from 1 μg total RNA using Taqman Reverse transcription reagents. qPCR was performed using Power SYBR Green PCR Master Mix and the detection was carried out in a 7500 Fast Real-Time PCR System (Applied Biosystems, PT). After amplification, melting curves were acquired and used to determine the specificity of PCR products, which were further confirmed using conventional gel electrophoresis. Quantification of IL-6 and TNFα genes was calculated relative to the expression of corresponding housekeeping gene GAPDH, according to the delta-delta Ct method. Primer sequences are shown in Table 2 of supplementary data 1.

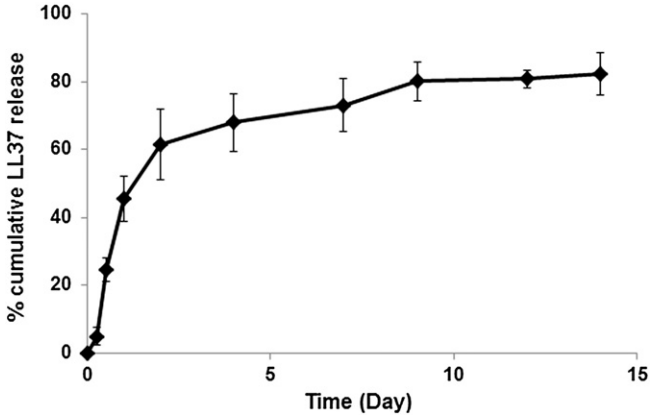

Fig. 1. *In vitro* release of LL37 (plotted as a function of % cumulative release vs time) from PLGA-LL37 NP (mean ± SD, $n = 3$).

2.9.5. Antimicrobial activity

LL37 (1, 2.5, 5 μg/ml), PLGA NP and PLGA-LL37 NP (1, 2.5, 5 mg/ml) were evaluated against 10^5 *E. coli* bacteria in 1 ml of PBS and incubated for 6 h at 37 °C. Aliquots (100 μl) were taken from the respective suspensions, diluted in PBS to give 10^3 bacteria per ml and plated on LB agar plates followed by incubation at 37 °C. Colonies were counted after 24 h of incubation.

2.10. Statistical analysis

The data are presented as mean ± SD. Statistical analysis was performed by using one-way ANOVA with the Tukey's test applied post hoc for paired comparisons of means (GraphPad Prism 5.0). Values of $p < 0.05^*$ and $p < 0.01^{**}$ were indicative of statistically significant differences.

3. Results

3.1. Preparation, characterization, release and stability studies of PLGA-LL37 NP

PLGA-LL37 NP were prepared by double (W/O/W) emulsion–solvent evaporation technique using PVA as stabilizer. The size, PDI, zeta potential and encapsulation efficiency of PLGA-LL37-NP are presented in Table 1.

PLGA-LL37 NP were stable and showed no significant differences in properties such as size, zeta potential and drug loading (quantified by

Table 1
Properties of PLGA-LL37 NP and PLGA NP (mean ± SD, $n = 4$).

Name	Particle size (nm)	Poly dispersity index	Zeta potential (mV)	Encapsulation efficiency (%)	Drug loading (μg LL37/mg PLGA NP)
PLGA-LL37 NP	304.5 ± 10.0	0.18 ± 0.01	−21.0 ± 2.5	70.2 ± 3.3	1.02 ± 0.06
PLGA NP	163.0 ± 2.2	0.15 ± 0.05	−19.2 ± 2.5	NA	NA

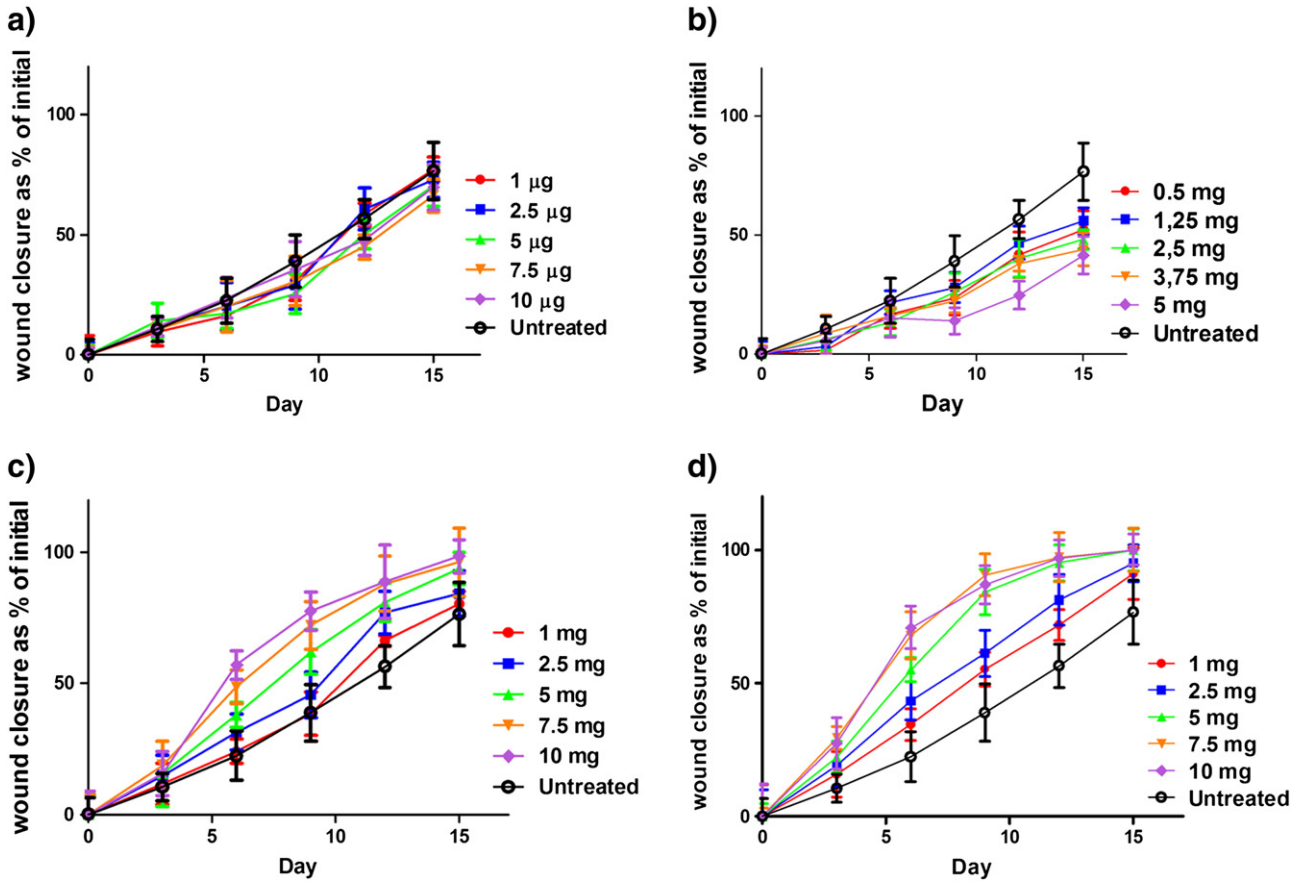

Fig. 2. Dose–response curve of different controls and PLGA-LL37 NP for wound healing activity: (a) LL37, (b) D,L lactic acid, (c) PLGA-NP and (d) PLGA-LL37 NP (mean ± SD; $n = 10$).

LC-ESI-MS) after 30 days of storage at room temperature (Table 1 of supplementary data 2). The *in vitro* drug release profile of LL37 from PLGA-LL37 NP was measured for 14 days (Fig. 1). Nearly 40% LL37 was detected in the supernatant after pelleting the NP within day 1 indicating that there was an initial burst release of LL37 from PLGA-LL37 NP and the release thereafter was approximately sustained. 80% of LL37 was released by day 14. Lactate release from PLGA-LL37 NP gradually increased and a 3 fold release was observed by day 15 when compared to day 5 (data not shown).

3.2. In vivo wound healing assay

3.2.1. Dose–response curves of LL37, lactic acid, PLGA NP and PLGA-LL37 NP

LL37, D,L-lactic acid, PLGA NP and PLGA-LL37 NP were evaluated for *in vivo* wound healing in a splinted mouse full thickness excisional model to plot the dose–response curves (Fig. 2). Increasing the dose of the LL37 peptide showed no significant change in activity whereas wounds treated with lactic acid showed delayed healing and necrosis at higher doses. With the increase in the lactic acid dose the condition of wounds was deteriorated. PLGA NP and PLGA-LL37 NP showed an enhanced wound closure with the increasing amount of NP. This was true until 7.5 mg/wound treatment and thereafter no significant increase was observed at higher doses. From day 10 onward, there were no differences observed between 5, 7.5 and 10 mg treated groups of PLGA-LL37 NP.

3.2.2. PLGA-LL37 NP promoted dermal wound healing

Based on the dose–response curves of PLGA-LL37 NP, 5 mg PLGA-LL37 NP/wound was chosen to understand the combined mechanisms of action of PLGA and LL37. Untreated (vehicle), 5 µg LL37, 5 mg PLGA NP and gene therapy of phCAP18/LL37 (pLL37) [18] by electroporation served as controls (Fig. 3a). Mice treated with PLGA-LL37 NP showed a significantly faster wound closure than those of untreated, LL37 and PLGA NP groups with 51 ± 4.9% versus 24 ± 3.0% for untreated versus 64.3 ± 4.8% for pLL37 at day 5 (Fig. 3b). The acceleration of wound healing by PLGA-LL37 NP became highly significant on days 7 and 10 showing an average healing of 79 ± 3.5% and 90 ± 4.5% respectively (Fig. 3c). Similar to the pLL37 treated group, by day 13 of post wounding the PLGA-LL37 NP treated group showed nearly complete wound closure whereas mice with LL37 and PLGA NP treated recovered by 75.0% at most. From day 7 of post wounding PLGA NP showed a faster healing effect than LL37 and untreated groups.

3.3. PLGA-LL37 NP showed higher re-epithelialization and granulation tissue formation

Histological examination of skin sections with HE and MT staining presented insights into the morphology of skin layers and collagen extent during the healing processes. On days 5 and 10, compared to all other groups, the PLGA-LL37 NP treated group showed a significant healing response similar to that of pLL37 group. In untreated, LL37 and PLGA NP groups, the granulation tissues formed were hypocellular and covered by a thin immature epithelium. It was clearly visible that in PLGA-LL37 NP and pLL37 groups, the epidermal and subepidermal layers were well organized. (Fig. 4a HE) By day 10 post wounding all groups showed better granulation tissue formation, re-epithelialization and dermal remodeling compared to the untreated group. Both MT staining and Sircol-collagen assay results revealed that the extent of collagen deposition was significantly higher in PLGA-LL37 NP and pLL37 groups

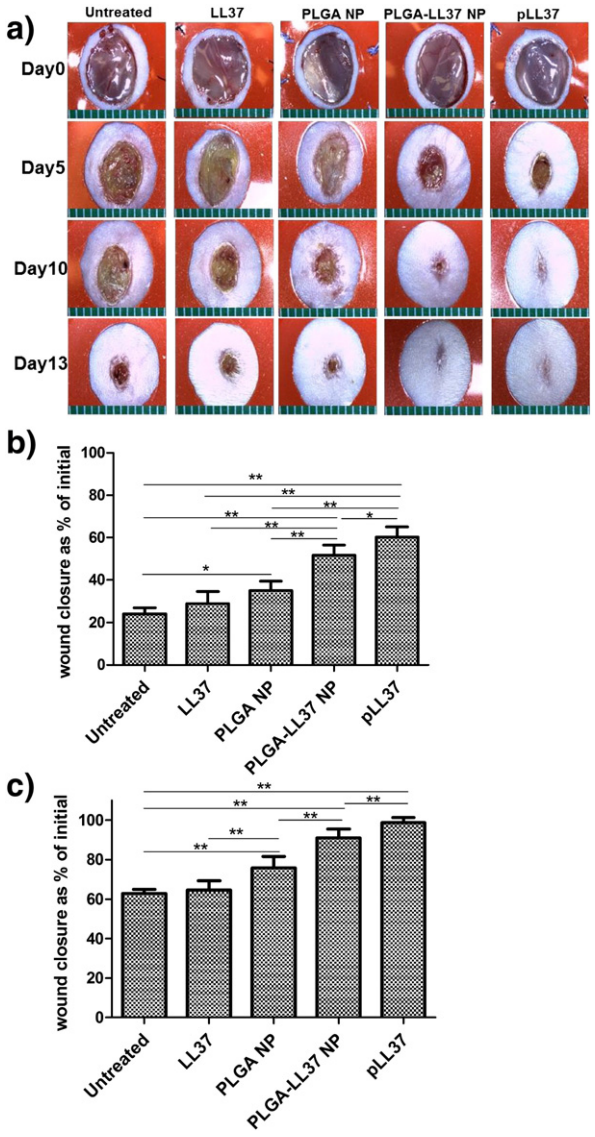

Fig. 3. PLGA-LL37 NP accelerate wound healing. (a) Representative images of wounds of five tested groups: Untreated, LL37, PLGA-NP, PLGA-LL37 NP and pLL37. Ruler units in mm. Wound area at (b) day 5 ($n = 13$) and (c) day 10 ($n = 10$) (mean ± SD).

and the deposited collagen showed a compact and denser alignment (Fig. 4a MT, b).

3.4. PLGA-LL37 NP up-regulated the expression of IL-6 and VEGFa and accelerated angiogenesis

IL-6 and VEGF expression plays an important role in wound healing processes. IL-6 modulates immune responses and is essential for timely wound healing [22] and vascular endothelial growth factor (VEGF) functions as an endothelial cell mitogen, chemotactic agent, and inducer of vascular permeability [23]. In order to check IL-6 and VEGFa expression during wound healing, we evaluated their relative mRNA expression in wound tissues of untreated and treated groups (LL37, PLGA NP, PLGA-LL NP and pLL37) on both post wounding day 5 (data not shown) and day 10 (Fig. 5a). q-PCR analysis revealed the significant higher expression of IL-6 and VEGFa on both days in PLGA-LL37 NP and pLL37 groups. Significantly, more CD31 + endothelial cells were detected in the section of PLGA-LL37 NP and pLL37 treated wounds (Fig. 5b, c) compared with all the other groups. No significant difference was observed between untreated, LL37 and PLGA NP treated groups.

3.5. PLGA-LL37 NP decreased myeloperoxidase activity

Azurophilic granules of neutrophils contain myeloperoxidase (MPO) and can be used as a quantitative index of inflammatory infiltration [21, 24]. As shown in Fig. 6, on day 5, compared to all the other groups, LL37 ($p < 0.05$) and pLL37 ($p < 0.01$) treatment showed a significant reduction of MPO enzymatic activity in the wound tissues. On day 10 of post wounding only PLGA-LL37 NP ($p < 0.05$) and pLL37 ($p < 0.01$) treated groups showed significantly lower MPO activity compared to the untreated, LL37 and PLGA NP groups.

3.6. Effects of PLGA-LL37 NP on HaCaT cells, BJ fibroblasts, macrophages and E. coli

HaCaT cells were cultured in the presence of cell media of concentrations 500 ng/ml LL37, 500 μg/ml PLGA NP and 500 μg/ml PLGA-LL37 NP and assays were performed for cell proliferation, migration and cytotoxicity. After 4 days, HaCaT and BJ fibroblast cells were analyzed for DNA quantification. At the tested concentration, no formulation showed a statistically significant effect on cell proliferation compared to control (Fig. 7a).

The effects of LL37, PLGA NP and PLGA-LL37 NP on the migratory capacity of HaCaT cells were determined by their ability to induce *in vitro* wound closure. The closure of wounds made in the confluent cell monolayers was tracked over 24 h (Fig. 7b, c). As the time of experiment was short, proliferation of cells may not affect the closure rate. Cells treated with LL37 showed a faster migration than those treated with PLGA-LL37 NP in the first few hours whilst PLGA-LL37 NP showed an equivalent migration effect at later time. By 12 h post-wounding, LL37 and PLGA-LL37 NP significantly improved closure of *in vitro* wounds compared to the control and PLGA NP. From this point on, *in vitro* wound closure in LL37 and PLGA-LL37 NP groups was statistically equivalent. MTT and LDH assays showed that the treatment of cells with the given dose of LL37, PLGA NP and PLGA-LL37 NP did not induce any cytotoxic effect on keratinocytes (data not shown). Macrophage cells treated with 300 μg of PLGA-LL37 NP showed a significant up-regulation of the mRNA expression of IL-6 versus untreated cells or cells treated with

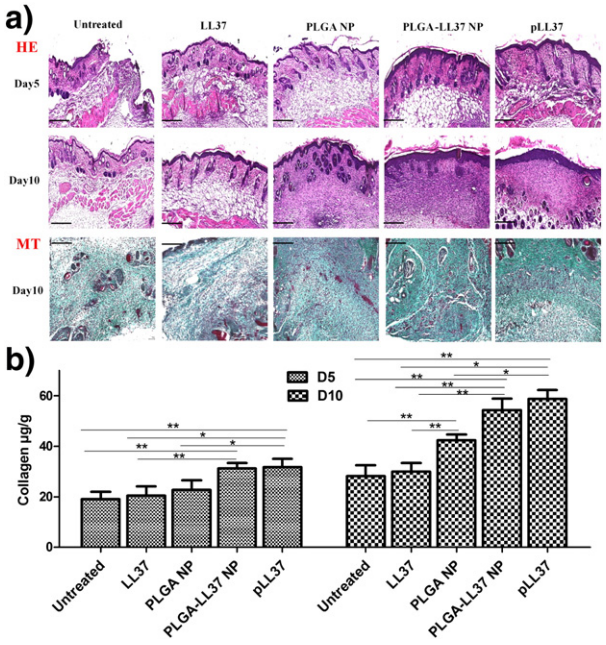

Fig. 4. PLGA-LL37 NP increased wound re-epithelialization and collagen content of granulation tissue. Wound sections ($n = 3$) were stained with (a) hematoxylin and eosin (HE) and Masson's trichrome (MT). Representative images of sections are presented for all five groups. Scale bar = 200 μm. (b) Sircol assay of collagen amounts in skin lysates of days 5 and 10 post wounding (mean ± SD; $n = 3$).

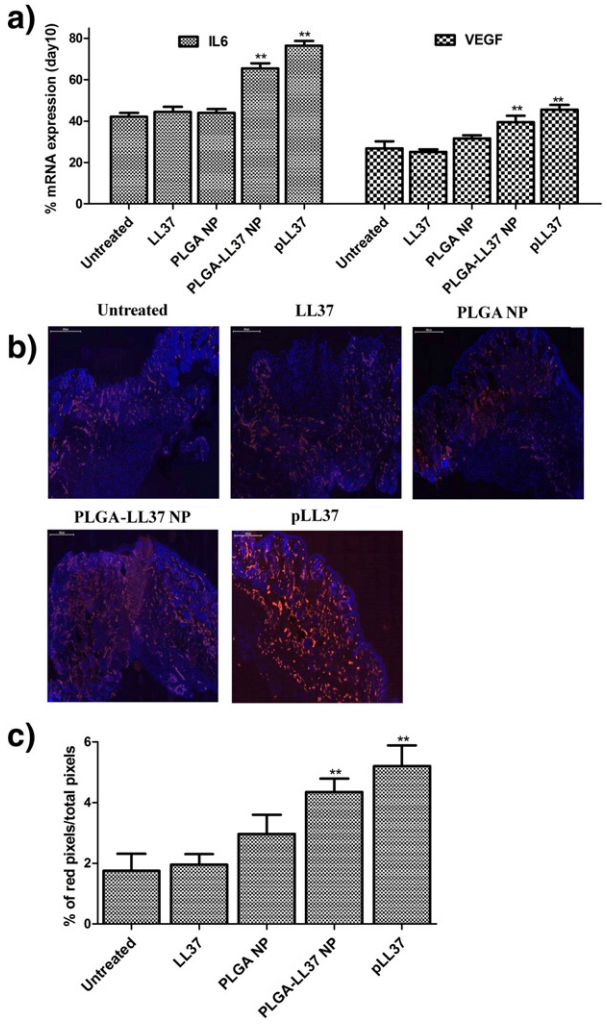

Fig. 5. a) *In vivo* quantitative determination of IL-6 and VEGFa transcription by q-PCR (day 10), b) representative pictures of IHC staining of endothelial cell marking with anti-CD 31 antibody (day 10), and c) quantification of red pixels representing the extent of CD31 marking (mean ± SD, $n = 3$). Statistical significance compared with the untreated group.

the LL37 and PLGA NP (Fig. 8a). Cells treated with LL37, PLGA NP and PLGA-LL37 NP showed a down-regulation of TNFα transcription versus untreated cells (Fig. 8b). The antimicrobial activity of LL37, PLGA NP and PLGA-LL37 NP was evaluated against 10^5 Gram-negative (*E. coli*) bacteria. LL37 peptide (5 μg/ml) and PLGA-LL37 NP (5 mg/ml) killed ~50% and ~25% of bacteria respectively. PLGA NP had no significant antimicrobial activity (Fig. 9).

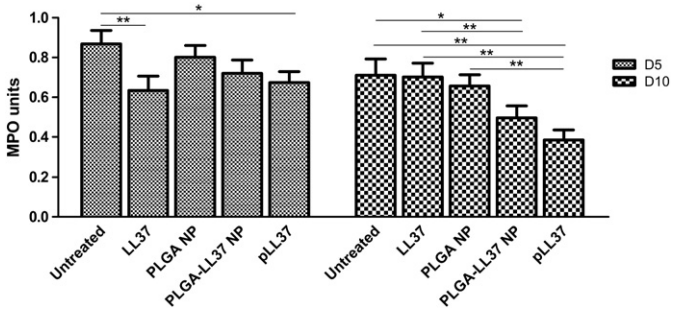

Fig. 6. MPO activity in differently treated wounded tissues on days 5 and 10 of post wounding (mean ± SD, $n = 3$).

4. Discussion

Various delivery systems have been developed to provide controlled release of proteins and peptides. However, clinical translation of these systems has been discouraged by their drawbacks such as poor loading and low biocompatibility of delivery systems. But, PLGA NP protect the loaded cargo from external environment and thereby enhance its availability and activity. Particularly its active involvement in wound healing processes is highly appropriate in the choice of delivery systems for wound treatment [5,13].

PLGA-LL37 NP have been prepared by using the W/O/W double emulsion–solvent evaporation technique that resulted in particles with high LL37 encapsulation (~70%) with a size of ~300 nm. The W/O/W double emulsion method offers protection to the peptide and is also one of the most appropriate methods to incorporate proteins in the nanoparticles. However, emulsification of the aqueous protein solution in an organic solvent such as methylene dichloride can be a deleterious step in the encapsulation process. In addition, factors such as speed and time of homogenizations, sonication and interaction of the protein molecule with organic solvent and/or polymer also determine the entrapment efficiency [25, 26]. At room temperature, PLGA-LL37 NP were stable. *In vitro* drug release of LL37 and lactate from PLGA-LL37 NP was performed. The LC-ESI-MS showed that the peptide was intact, chemically unmodified and stable. LL37 release profile followed a biphasic

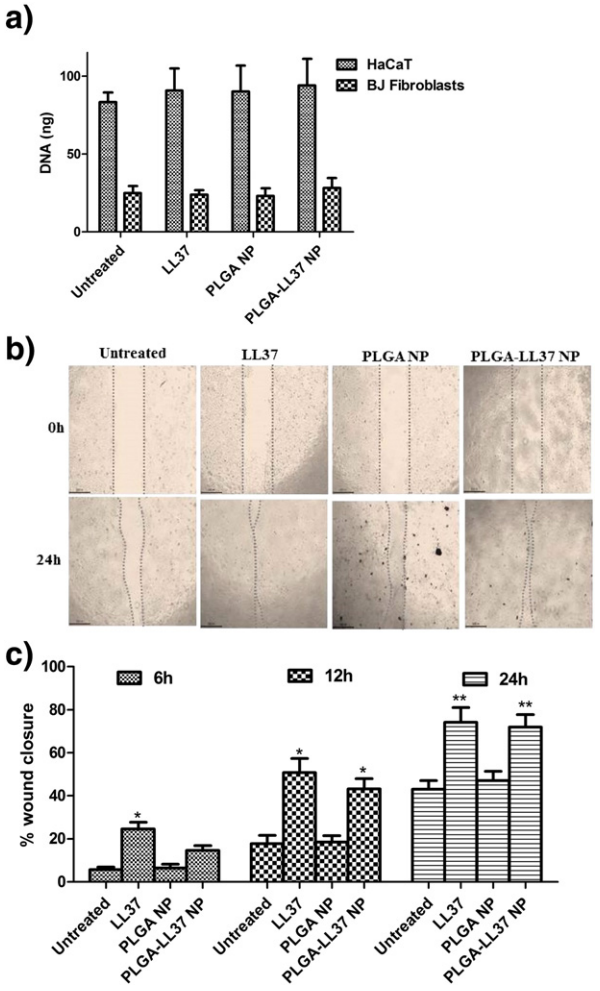

Fig. 7. *In vitro* evaluation of PLGA-LL37 NP. (a) DNA quantification of HaCaT cells and BJ fibroblasts after 4 day incubation with formulations (mean ± SD, $n = 4$). (b) Effect of LL37, PLGA NP and PLGA-LL37 NP on migration of HaCaT cells was assessed by IBIDI wound healing assay. (c) Results are expressed as percentage of initial wound (mean ± SD; $n = 4$). Statistical significance compared with the untreated group.

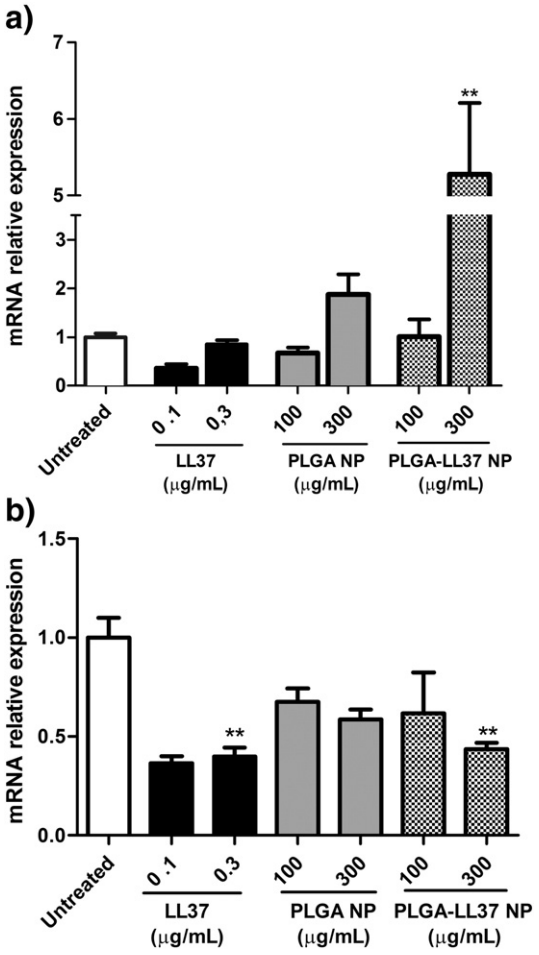

Fig. 8. *In vitro* quantitative determination of a) IL-6 and b) TNFα expression at mRNA level in macrophages (mean ± SD; $n = 3$). Statistical significance compared with the untreated group.

pattern with an initial burst followed by slow and sustained release (Fig. 1). The initial burst release of LL37 (~40% within day 1) is also appropriate for the activity of LL37 in wound healing. Measurements also showed that the PLGA served as a sustained source of lactate. The release of lacatate and the loaded drug may be accelerated *in vivo*, driven by additional enzymatic activity in the wound bed. Indeed, the *in vivo* degradation of PLGA is mainly due to water absorption, pore formation and enzymatic activities for the hydrolysis of intra-polymer linkages and auto-catalysis leading to erosion [27].

Different doses of LL37, lactic acid, PLGA NP and PLGA-LL37 NP formulations were tested for *in vivo* wound healing to plot the dose–response curves and determine the rational dose. Lack of activity in case of LL37 peptide, deterioration of wounds condition in case of lactic acid and greater healing than PLGA NP, demonstrated that the utilization of PLGA NP as a carrier for LL37 fastened the healing processes. Among the different doses of PLGA-LL37 NP, 5 mg was selected as rational dose as it was as efficient as 7.5 and 10 mg doses (Fig. 2). Mechanistic approaches were established with a further *in vivo* testing. By performing *in vivo* experiments with all five groups (untreated, LL37, PLGA NP, PLGA-LL37 NP and pLL37) we attempted to present a comprehensive comparative validation of their potential to promote wound healing (Fig. 3). Wound area measurements clearly showed that PLGA-LL37 NP and pLL37 treated mice exhibited a significant faster wound closure than the other groups. Accelerated wound healing by PLGA-LL37 NP became highly significant from day 7 and by the day 13 PLGA-LL37 NP induced nearly complete wound closure. Compared to untreated negative controls, the PLGA NP treatment displayed its beneficial add on effect of sustained lactate release to the wounds by significant accelerated healing. Accordingly, PLGA-LL37 NP accelerated healing more significantly than LL37 and PLGA NP, thus supporting the hypothesis of combined effects of encapsulated LL37 and lactate. Moreover, the wound healing effect of PLGA-LL37 NP was very much similar to that of gene therapy using pLL37.

To establish the mechanisms, wound tissues were collected on days 5 and 10 for histological and biochemical analysis. Histological examination of skin sections with HE and MT staining presented insights on the morphology of skin layers and collagen extant during the healing processes. In the PLGA-LL37 NP treated groups, regenerated wound epithelium and subepidermal layers were well organized. Compared to the other groups, PLGA-LL37 NP and pLL37 treated mice showed advanced granulation tissue formation leading to more mature wound architecture. Deposited collagen showed a compact and denser alignment. Migration of keratinocytes into the wound bed is one of the main factors contributing to epidermal wound healing. Several soluble factors have been shown to influence keratinocyte migration, such as TGF-β and cytokines like IL-6 [28]. LL37 delivered by PLGA-LL37 NP and pLL37 electroporation accelerated keratinocyte migration and fastened re-epithelialization leading to accelerated maturation of a thicker neoepidermal layer visible on the histological (HE) sections on days 5 and 10 after treatment (Fig. 4a). These results were confirmed by our findings in the *in-vitro* migration assay (Fig. 7b, c). The amount of collagen deposition indicates the activity of fibroblasts in the new formed granulation tissue, a prerequisite step during the proliferation and remodeling phase of wound healing. By up-regulating IL-6 expression, LL37 activates epidermal cells and fibroblasts to form granulation tissue, and acts as a chemo-attractant to macrophages and fibroblasts [29]. In a feedback mechanism, LL37 from activated leukocytes has shown a direct influence on dermal fibroblasts by increasing the synthesis of the extracellular matrix proteoglycans that are required for the activity of many growth factors. IL-6 may also induce collagen deposition indirectly by induction of *TGF-β* gene expression. In addition, lactate in wounds is a major signal for collagen synthesis and wound repair [30]. PLGA-LL37 NP treated wounds clearly achieved greater re-epithelialization and collagen content due to the mechanisms of action of both LL37 and lactate in wound healing [4,10,31].

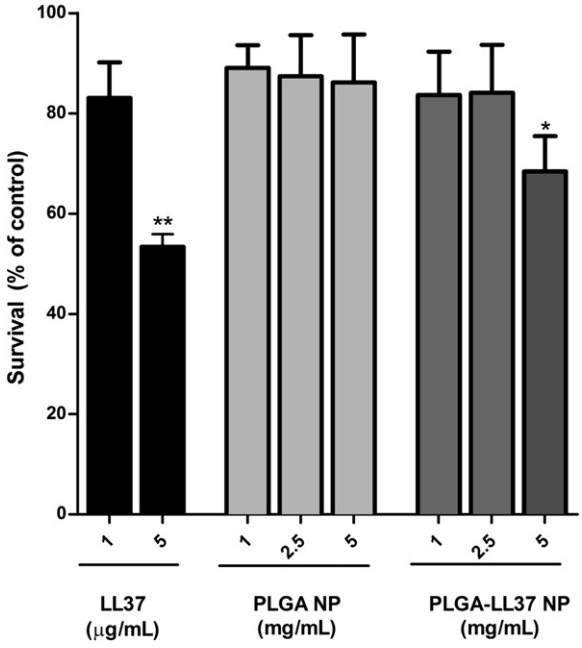

Fig. 9. Antimicrobial activity of LL37, PLGA NP and PLGA-LL37 NP against 10^5 *E. coli* cells per ml (mean ± SD; $n = 3$). Statistical significance compared with the untreated group.

IL-6 and VEGFa expression plays an important role in wound healing processes. PLGA-LL37 NP promoted the expression of IL-6 and VEGFa mRNA (Fig. 5a). Interestingly, it was previously shown known that LL37 can induce the expression of chemokines and chemokine receptors such as IL-6, IL-8, GM-CSF, IL-10, interferon-inducible protein-10 (IP-10), monocyte chemotactic protein-1 (MCP-1), *etc.* in macrophages. Thus, by indirectly promoting the migration of immune cells, LL37 contributes to the immune response against infection. There was definitive evidence that IL-6 has crucial roles in the wound healing process by regulating leukocyte infiltration, angiogenesis, and collagen deposition [18]. Our *in vivo* results recapitulate changes in *in vitro* IL-6 expression. By inhibiting the activation, LL37 also reduces the TNFα expression in mouse macrophage cells (Fig. 8a, b) [32,33]. IL-6 can further induce angiogenesis by inducing VEGF production. Also, Lin *et al.* have shown that VEGF gene expression was reduced at wound sites of IL-6 knockout mice compared with wild type mice [34]. This clearly suggests that there can be a relation between the VEGF and IL-6 up-regulation effects of LL37. In addition, high lactate levels also cause a decline in the post-translational poly-ADP ribosylation (PAR) modification of VEGF, which renders VEGF biologically more active [35]. PLGA-LL37 NP treated groups showed a higher immunohistochemistry (CD31 +) staining of endothelial cells in wound tissue sections (Fig. 5b, c). Thus, PLGA-LL37 NP treated wounds exhibited up-regulation of IL-6 and VGEFa transcription and greater angiogenesis because of the combined effects of LL37 and lactate.

During natural wound healing LL37 concentrations are typically found at sites of inflammation, where they act as primary defense against bacteria and other pathogens. In the very early stage of inflammation (24–48 h post wounding) LL37 acts as a chemo-attractant and triggers the infiltration of leucocytes toward the wound. Infiltered neutrophils produce and respond to LL-37 building up high concentrations of LL37 at the wound site. This 'burst' of LL-37 enables a potent immune response, capable of rapidly resolving the infection [36]. At 3–5 days of post wounding, LL37 markedly reduced MPO activity and was actively involved in the remodeling of wound layers [8]. MPO is an enzyme mostly found in neutrophils and that can be used as a quantitative index of inflammatory infiltration in wounds [24]. In our study, only LL37 and pLL37 treated wounds showed significant reduced MPO activity on day 5 post treatment, whereas on day 10 PLGA-LL37 NP and pLL37 treated groups showed significantly less MPO activity (Fig. 6). The explanation for this result could be found in the different pharmacokinetic but equal pharmacodynamic responses in the wounds. LL37 and pLL37 treatments achieved pharmacokinetic relevant initial levels of LL37 to reduce the MPO activity at the early stage of wound healing, whereas only the released LL37 from PLGA-LL37 NP and pLL37 electroporation resulted in a significant late immunomodulation with reduced MPO activity, indicating a successful reduction of wound inflammation. Down-regulation of the expression of TNFα mRNA in activated macrophages also supports the immunomodulation activities of LL37 and its involvement in inflammatory pathways.

In order to understand the cellular mechanisms involved in the LL37 wound healing activities, *in vitro* proliferation, migration and cytotoxicity assays were performed (Fig. 7). Although there was no proliferation effect of formulations at the given concentration on HaCaT cells and BJ fibroblasts, it is evident that LL37 peptide is readily available in the medium which induced a conversion of HaCaT cells to a migratory phenotype with numerous filopodia-like protrusions of the plasma membrane, which resulted in an enhancement of cell migration [37]. MTT and LDH assays showed that the treatment of HaCaT cells with the given dose of LL37, PLGA NP and PLGA-LL37 NP did not induce any cytotoxic effect. LL37 and PLGA-LL37 NP showed antimicrobial activity on *E.coli*. According to the release studies, PLGA-LL37 NP released ~30% of LL37 within 6 h and therefore the released LL37 may explain the lower antimicrobial activity compared to LL37 peptide treated bacteria (Fig. 9).

Thus, different mechanisms of PLGA-LL37 NP accelerated the wound closure by targeting different phases of wound healing. Hence, the discussed results justified the use of PLGA and LL37 combination in wound healing therapy.

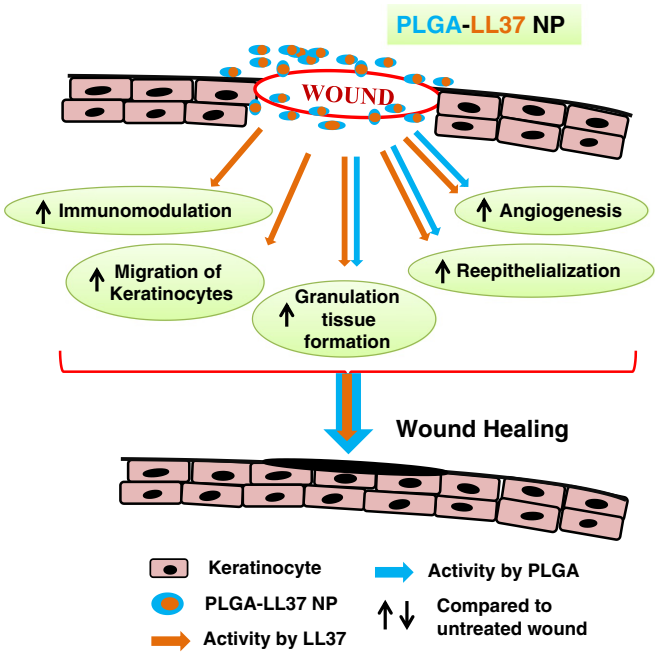

Scheme 1. Schematic representation of mechanisms of action of LL37 and PLGA (lactate) in wound healing processes.

5. Conclusions

Administration of LL37 in PLGA nanoparticles and combined therapeutic activities of PLGA and LL37 to fasten dermal wound healing were investigated in the current study (Scheme 1). We demonstrated that the PLGA-based sustained delivery of LL37 significantly improved the wound healing activity compared to PLGA or LL37 alone. The healing effect of PLGA-LL37 NP included higher re-epithelialization, granulation tissue formation and immunomodulation. PLGA-LL37 NP significantly up-regulated IL-6 and VEGFa at mRNA level and improved angiogenesis. These results established that PLGA-based drug delivery systems can promote wound healing activities because of both sustained release of bioactive LL37 and the intrinsic lactate activity.

Supplementary data to this article can be found online at http://dx.doi.org/10.1016/j.jconrel.2014.08.016.

Acknowledgments

The financial support (grant agreement number 289454) from the European Commission and Marie Curie Actions is greatly appreciated. We express our earnest thanks to Mr. Bernard Ucakar (Louvain Drug Research Institute, UCL, BE) and Mr. Raoul Rozenberg (Institute of Condensed Matter and Nanosciences, UCL, BE) for their help with animal experiments and mass spectrometry measurements respectively. Kiran Kumar Chereddy, Michela Comune and Claudia Moia are early stage researchers (ESR) of FP7 Marie Curie NANODRUG network. Gaëlle Vandermeulen is postdoctoral researchers of the Belgian Fonds National de la Recherche Scientifique (FRS-FNRS).

References

[1] M.G. Franz, M.C. Robson, D.L. Steed, A. Barbul, H. Brem, D.M. Cooper, D. Leaper, S.M. Milner, W.G. Payne, T.L. Wachtel, L. Wiersema-Bryant, Guidelines to aid healing of acute wounds by decreasing impediments of healing, Wound Repair Regen. 16 (2008) 723–748.

[2] C.K. Sen, G.M. Gordillo, S. Roy, R. Kirsner, L. Lambert, T.K. Hunt, F. Gottrup, G.C. Gurtner, M.T. Longaker, Human skin wounds: a major and snowballing threat to public health and the economy, Wound Repair Regen. 17 (2009) 763–771.
[3] C.L. Baum, C.J. Arpey, Normal cutaneous wound healing: clinical correlation with cellular and molecular events, Dermatol. Surg. 31 (2005) 674–686.
[4] P.E. Porporato, V.L. Payen, C.J. De Saedeleer, V. Preat, J.P. Thissen, O. Feron, P. Sonveaux, Lactate stimulates angiogenesis and accelerates the healing of superficial and ischemic wounds in mice, Angiogenesis 15 (2012) 581–592.
[5] F. Danhier, E. Ansorena, J.M. Silva, R. Coco, A. Le Breton, V. Préat, PLGA-based nanoparticles: an overview of biomedical applications, J. Control. Release 161 (2012) 505–522.
[6] W. Acampa, M. Petretta, L. Evangelista, S. Daniele, E. Xhoxhi, M.L. De Rimini, C. Cittanti, F. Marranzano, M. Spadafora, S. Baldari, L. Mansi, A. Cuocolo, Myocardial perfusion imaging and risk classification for coronary heart disease in diabetic patients. The IDIS study: a prospective, multicentre trial, Eur. J. Nucl. Med. Mol. Imaging 39 (2012) 387–395.
[7] M. Frohm, H. Gunne, A.-C. Bergman, B. Agerberth, T. Bergman, A. Boman, S. Lidén, H. Jörnvall, H.G. Boman, Biochemical and antibacterial analysis of human wound and blister fluid, Eur. J. Biochem. 237 (1996) 86–92.
[8] D. Vandamme, B. Landuyt, W. Luyten, L. Schoofs, A comprehensive summary of LL-37, the factotum human cathelicidin peptide, Cell. Immunol. 280 (2012) 22–35.
[9] M. Frohm, B. Agerberth, G. Ahangari, M. Ståhle-Bäckdahl, S. Lidén, H. Wigzell, G.H. Gudmundsson, The expression of the gene coding for the antibacterial peptide LL-37 is induced in human keratinocytes during inflammatory disorders, J. Biol. Chem. 272 (1997) 15258–15263.
[10] L. Steinstraesser, T. Koehler, F. Jacobsen, A. Daigeler, O. Goertz, S. Langer, M. Kesting, H. Steinau, E. Eriksson, T. Hirsch, Host defense peptides in wound healing, Mol. Med. 14 (2008) 528–537.
[11] R. Ramos, J.P. Silva, A.C. Rodrigues, R. Costa, L. Guardao, F. Schmitt, R. Soares, M. Vilanova, L. Domingues, M. Gama, Wound healing activity of the human antimicrobial peptide LL37, Peptides 32 (2011) 1469–1476.
[12] M. Carretero, M. del Río, M. García, M.J. Escámez, I. Mirones, L. Rivas, C. Balague, J.L. Jorcano, F. Larcher, A cutaneous gene therapy approach to treat infection through keratinocyte-targeted overexpression of antimicrobial peptides, J. Fed. Am. Soc. Exp. Biol. 18 (15) (2004) 1931–1933.
[13] D.S. Pisal, M.P. Kosloski, S.V. Balu-Iyer, Delivery of therapeutic proteins, J. Pharm. Sci. 99 (2010) 2557–2575.
[14] J.S. Golub, Y.-t. Kim, C.L. Duvall, R.V. Bellamkonda, D. Gupta, A.S. Lin, D. Weiss, W. Robert Taylor, R.E. Guldberg, Sustained VEGF delivery via PLGA nanoparticles promotes vascular growth, Am. J. Physiol. Heart Circ. Physiol. 298 (2010) H1959–H1965.
[15] M. Chacón, J. Molpeceres, L. Berges, M. Guzmán, M.R. Aberturas, Stability and freeze-drying of cyclosporine loaded poly(d, l lactide–glycolide) carriers, Eur. J. Pharm. Sci. 8 (1999) 99–107.
[16] N.R. Johnson, Y. Wang, Controlled delivery of heparin-binding EGF-like growth factor yields fast and comprehensive wound healing, J. Control. Release 166 (2013) 124–129.
[17] K.K. Chereddy, R. Coco, P.B. Memvanga, B. Ucakar, A. des Rieux, G. Vandermeulen, V. Préat, Combined effect of PLGA and curcumin on wound healing activity, J. Control. Release 171 (2013) 208–215.
[18] L. Steinstraesser, M.C. Lam, F. Jacobsen, P.E. Porporato, K.K. Chereddy, M. Becerikli, I. Stricker, R.E.W. Hancock, M. Lehnhardt, P. Sonveaux, V. Preat, G. Vandermeulen, Skin electroporation of a plasmid encoding hCAP-18/LL-37 host defense peptide promotes wound healing, Mol. Ther. 22 (2013) 734–742.
[19] A. des Rieux, B. Ucakar, B.P.K. Mupendwa, D. Colau, O. Feron, P. Carmeliet, V. Préat, 3D systems delivering VEGF to promote angiogenesis for tissue engineering, J. Control. Release 150 (2011) 272–278.
[20] E. Olaso, H.-C. Lin, L.-H. Wang, S. Friedman, Impaired dermal wound healing in discoidin domain receptor 2-deficient mice associated with defective extracellular matrix remodeling, Fibrogenesis Tissue Repair 4 (2011) 5.
[21] Peter P. Bradley, Dennis A. Priebat, R.D.C., G. Rothstein, Measurement of cutaneous inflammation: estimation of neutrophil content with an enzyme marker, J. Investig. Dermatol. (1982) 206–209.
[22] M.M. McFarland-Mancini, H.M. Funk, A.M. Paluch, M. Zhou, P.V. Giridhar, C.A. Mercer, S.C. Kozma, A.F. Drew, Differences in wound healing in mice with deficiency of IL-6 versus IL-6 receptor, J. Immunol. 184 (2010) 7219–7228.
[23] D.W. Leung, G. Cachianes, W.J. Kuang, D.V. Goeddel, N. Ferrara, Vascular endothelial growth factor is a secreted angiogenic mitogen, Science 246 (1989) 1306–1309.
[24] A. Hasmann, E. Wehrschuetz-Sigl, A. Marold, H. Wiesbauer, R. Schoeftner, U. Gewessler, A. Kandelbauer, D. Schiffer, K.P. Schneider, B. Binder, M. Schintler, G.M. Guebitz, Analysis of myeloperoxidase activity in wound fluids as a marker of infection, Ann. Clin. Biochem. 50 (2013) 245–254.
[25] E.G.G. Spada, P. Giunchedi, Protein delivery from polymeric nanoparticles, World Acad. Sci. Eng. Technol. 52 (2011) 245–249.
[26] M.D. Blanco, M.J. Alonso, Development and characterization of protein-loaded poly(lactide-co-glycolide) nanospheres, Eur. J. Pharm. Biopharm. 43 (1997) 287–294.
[27] S. Fredenberg, M. Wahlgren, M. Reslow, A. Axelsson, The mechanisms of drug release in poly(lactic-co-glycolic acid)-based drug delivery systems—a review, Int. J. Pharm. 415 (2011) 34–52.
[28] P. Martin, Wound healing—aiming for perfect skin regeneration, Science 276 (1997) 75–81.
[29] R.M. Gallucci, D.K. Sloan, J.M. Heck, A.R. Murray, S.J. O'Dell, Interleukin 6 indirectly induces keratinocyte migration, J. Investig. Dermatol. 122 (2004) 764–772.
[30] T.K. Hunt, W.B. Conolly, S.B. Aronson, P. Goldstein, Anaerobic metabolism and wound healing: an hypothesis for the initiation and cessation of collagen synthesis in wounds, Am. J. Surg. 135 (1978) 328–332.
[31] O. Trabold, S. Wagner, C. Wicke, H. Scheuenstuhl, M.Z. Hussain, N. Rosen, A. Seremetiev, H.D. Becker, T.K. Hunt, Lactate and oxygen constitute a fundamental regulatory mechanism in wound healing, Wound Repair Regen. 11 (2003) 504–509.
[32] D.E. Owens Iii, N.A. Peppas, Opsonization, biodistribution, and pharmacokinetics of polymeric nanoparticles, Int. J. Pharm. 307 (2006) 93–102.
[33] M.G. Scott, D.J. Davidson, M.R. Gold, D. Bowdish, R.E.W. Hancock, The human antimicrobial peptide LL-37 is a multifunctional modulator of innate immune responses, J. Immunol. 169 (2002) 3883–3891.
[34] Z.-Q. Lin, T. Kondo, Y. Ishida, T. Takayasu, N. Mukaida, Essential involvement of IL-6 in the skin wound-healing process as evidenced by delayed wound healing in IL-6-deficient mice, J. Leukoc. Biol. 73 (2003) 713–721.
[35] V.B.S. Kumar, R.I. Viji, M.S. Kiran, P.R. Sudhakaran, Endothelial cell response to lactate: implication of PAR modification of VEGF, J. Cell. Physiol. 211 (2007) 477–485.
[36] O. Sørensen, K. Arnljots, J.B. Cowland, D.F. Bainton, N. Borregaard, The human antibacterial cathelicidin, hCAP-18, is synthesized in myelocytes and metamyelocytes and localized to specific granules in neutrophils, Blood 90 (1997) 2796–2803.
[37] M. Carretero, M.J. Escamez, M. Garcia, B. Duarte, A. Holguin, L. Retamosa, J.L. Jorcano, M.D. Rio, F. Larcher, In vitro and in vivo wound healing-promoting activities of human cathelicidin LL-37, J. Investig. Dermatol. 128 (2008) 223–236.